

# THE OBSERVATION OF REVERBERATION IN THE OCEAN BY ACOUSTIC COMBINED RECEIVER

VLADIMIR SHCHUROV, BENJAMIN DOROZHKO\* AND MARIANNA  
KUYANOVA

V.I. Il'ichev Pacific Oceanological Institute  
690041, 43, Baltiyskaya St., Vladivostok, Russia  
e-mail: Shchurov@poi.dvo.ru

\*Institute for Automation and Control Processes  
690041, 5, Radio St., Vladivostok, Russia  
e-mail: bendor@iacp.dvo.ru

*Results of observation of low-frequency tone pulse reverberation in deep open ocean by means of the combined sensor are presented. As the experiment showed, net energy flux density vector of the echo-signal carries information on properties of scattering directionality. The paper shows that the energy flux density vector of the field of surface – scattered low-frequency sound has both random and regular contributions. The regular contribution can be identified as the diffraction spectrum of scattered sound that is in line with the theory developed by L. Brekhovskikh. Lifetime of regular orderly structures existing in surface roughness is no less than 96 s as the experiment proves. The surface roughness diffraction lattice is likely to be built of swell waves.*

## INTRODUCTION

Sound reverberation in the ocean is in fact one of the issues providing knowledge of acoustic and oceanological properties of the ocean waveguide. Backscattering of the sound being a major contributor to reverberation has had an advanced study in numerous theoretical and experimental works. The paper presents simultaneous measurements of the pressure  $p(t)$  and the three orthogonal projections of the particle velocity  $V_x(t)$ ,  $V_y(t)$ , and  $V_z(t)$  made at the same point of the sound field, whereas all field deployments focused on sound backscattering used to employ just only sound pressure measurement so far. The measured characteristics enable to calculate orthogonal projections of the sound field energy flux density vector, the total vector of the energy flux density, and its azimuthal and elevation angles at a given point

of the ocean waveguide. The approach offered makes it possible to study an energy transport occurred in the reverberation field in the angular range of  $4\pi$ . Low-frequency sound scattering is of peculiar interest. As follows from theoretical works published by L. M. Brekhovskikh, sound diffraction at a sine surface roughness is similar to scattering at a diffraction lattice, see Refs. 1 and 2. Actual rough surface can be considered as a random diffraction lattice. On the basis of measurements of energy fluxes resulted from surface-scattered tone pulses an attempt was made to experimentally reveal a diffraction spectrum in the reverberation field.

## 1. DESCRIPTION OF THE EXPERIMENT

The measurements made in deep open waters of the South China Sea. The research ship “Academician M. Lavrent’ev” used for sound transmission was 3150 m apart from telemetric acoustic combined sensing system. The combined receiver of the telemetric system was positioned at the depth of 150 m. Cartesian frame of reference assigned to the combined receiver was arranged as follows, the x and y axes were in the horizontal plane, the z axis was vertical and directed from the surface to the bottom. Omnidirectional sound transmitter was at the depth of 50 m. Sounding 617-Hz tone pulses were 0.9 s long with time separation of 4 s. The transmission level converted for 1 m was 135 dB re  $1\mu\text{Pa}$ . The ambient noise level at 617 Hz scaled to units of pressure was 65 dB re  $1\mu\text{Pa}^2/\text{Hz}$ . The direct signal arrived at  $\varphi = -45^\circ$  with respect to x-axis and  $\theta = 85^\circ$  with respect to z-axis. Wind speeds were between 8 and 9 m/s, and wind direction was within the limits of  $\varphi \approx -(30^\circ-20^\circ)$ . Steady-state wind-driven waves with wave height of about 1.5 m and swell were observed. The deployment site depth was about 3800 m; underwater sound channel axis was at the depth of 1000 m. Sound speed at the surface was 7 m/s greater than that at the bottom. Another, relatively weak sound channel was also found in the near-surface upper layer, which was 60-m thick, see Tab. 1.

Tab.1 Station #ST0008; January 3, 1992; local time 08:34 a.m.;  
geographic coordinates:  $18^\circ 01' \text{ N}$ ,  $116^\circ 07' \text{ E}$ ; depth of the site 3800 m

depth (m)	sound speed (m/s)	depth (m)	sound speed (m/s)	depth (m)	sound speed (m/s)	depth (m)	sound speed (m/s)
0	1530.0	130	1515.5	500	1491.7	1300	1485.3
10	1530.1	140	1514.9	550	1490.3	1400	1486.0
20	1530.3	150	1513.3	600	1489.0	1500	1487.7
30	1530.4	160	1511.7	650	1487.6	1600	1487.7
40	1530.2	170	1510.5	700	1486.9	1600	1488.9
50	1530.4	180	1509.3	750	1486.4	1800	1490.2
60	1530.5	190	1507.7	800	1485.6	1900	1491.6
70	1530.2	200	1506.1	850	1485.4	2000	1493.2
80	1528.5	250	1501.5	900	1484.9	2250	1497.2
90	1525.2	300	1499.1	950	1484.7	2500	1501.3
100	1521.4	350	1496.1	1000	1484.7	2557	1502.2
110	1519.5	400	1494.8	1100	1484.7	3800	1523.0
120	1516.8	450	1493.6	1200	1484.9		

## 2. DATA PROCESSING

In the reverberation field combined sensor records the net energy flux of the total echo-signal every given instant all over the angle of  $4\pi$ . Once a diffusive contribution is inherent in the echo-signal, it is to be eliminated in cross-component data procession. Hence, the net energy flux of the echo-signal will be available. On the basis of this very peculiarity of combined sensing, a strategy for reverberation directional properties observation has been developed.

A sequence of 24 time series 4 s long each recorded at a depth of 150 m was used in data processing. Upon filtration, in the  $\pm 5$  Hz vicinity of the frequency of 617 Hz, energy flux density vector orthogonal projections have been estimated at every given moment over each time series 4 s long. Angles  $\varphi$  and  $\theta$  have been calculated from expressions presented in Ref. 3.

The echo-signal heading being described by a pair of angles  $\varphi$  and  $\theta$ , and time of arrival  $t$  at the measurement point was estimated from the analysis of a normalized mean number of echo-signals for a set of quantities  $\varphi_0$ ,  $\theta_0$ , and  $t_0$ . Horizontal characteristic of reverberation in the  $xOy$  plane was determined by the azimuthal angle  $\varphi$  and time of arrival  $t$ ; in the vertical plane by the elevation angle  $\theta$  and  $t$ . Available data sets of random  $\varphi$  and  $\theta$  at certain  $t$  were used to build a horizontal  $(\varphi, t)$  and a vertical  $(\theta, t)$  polar sonograms. A set of 24 time series 4 s long each was used in these calculations. Directional properties of reverberation can be judged from shapes of the sonograms. Then we made “sections” of the data collected in the horizontal sonogram  $(\varphi, t)$  sectors of interest with subsequent normalizing thereof. The profiles obtained were compared to corresponding elevation angles in sonograms  $(\theta, t)$  and used in building a 3-d “portrait” of reverberation in the measurement point in corresponding angular spatial sector.

Hence we coincide a polar frame of reference  $\varphi, \theta$ , and  $t$  with the Cartesian one associated with the combined sensor. Here the radius  $r$  is the time of arrival. The angle  $\varphi$  is measured from the  $x$ -axis and the angle  $\theta$  from the  $z$ -axis. In the horizontal plane  $2\pi$  is separated into a set of 10 or 20-deg sectors. Each of these horizontal sectors is associated with a vertical one in which  $\theta$  varies between 0 and  $\pi$ . While calculating  $\varphi$ , the experimental error was within  $\pm 5^\circ$  for 10-deg sectors and  $\pm 10^\circ$  for 20-deg sectors whereas it is  $\pm 5^\circ$  for  $\theta$  calculations.

## 3. RESULTS

Fig. 1 shows an oscillogram of one of 24 four-component time series recorded at a depth of 150 m. Frequency of the tone was 617 Hz, the analysis was made in 10-Hz frequency band. The transmitter appeared to be rather close to the surface that elongated the direct pulse up to 0.96 s due to the surface reflection. No direct pulse is seen in the  $V_z(t)$  oscillogram, instead one can observe a pulse scattered by a peace of the surface directly above the combined sensor. So the scattered pulse becomes trapped by the directivity pattern of  $z$ -channel.

Fig. 2 shows the reverberation sonogram in the horizontal plane that was built by collecting pulses of the scattered field over 24 independent time series. The arrivals were collected in 36 sectors, 10-deg each. As noted above, the radius in the sonogram is the length of the time series equal to 4 s, where  $t=0$  corresponds to the instant of the direct pulse arrival at the measurement point. As follows from the sonogram in Fig. 2, within the framework of the taken strategy in reverberation observation, echo-signals being a sum of scattered pulses

with certain  $\varphi_0$  and  $t_0$  show uneven distribution. At certain angles  $\varphi$  significant number of sequential echo-signals are observed whereas at another azimuths no signals are found. In the sonogram between 270 and 60 degrees bottom reverberation is observed. Echo-signal from the bottom arrives at the measurement point at  $t=3.41$  s that is in perfect agreement with the geometry of the deployment. Between  $t=0.96$  s and  $t=3.41$  s in the sonogram in Fig. 2 one can see surface and volume reverberation arrivals. While making a comparison between sonograms related to the vertical and horizontal angular sectors one can estimate directional properties of surface and volume scattering via following indication. Scattering caused by surface scatters arrives at the measurement point at angles  $\theta \leq \pi/2$ ; whereas scattering from volume scatters located in the waveguide interior does at angles  $\theta > \pi/2$ .

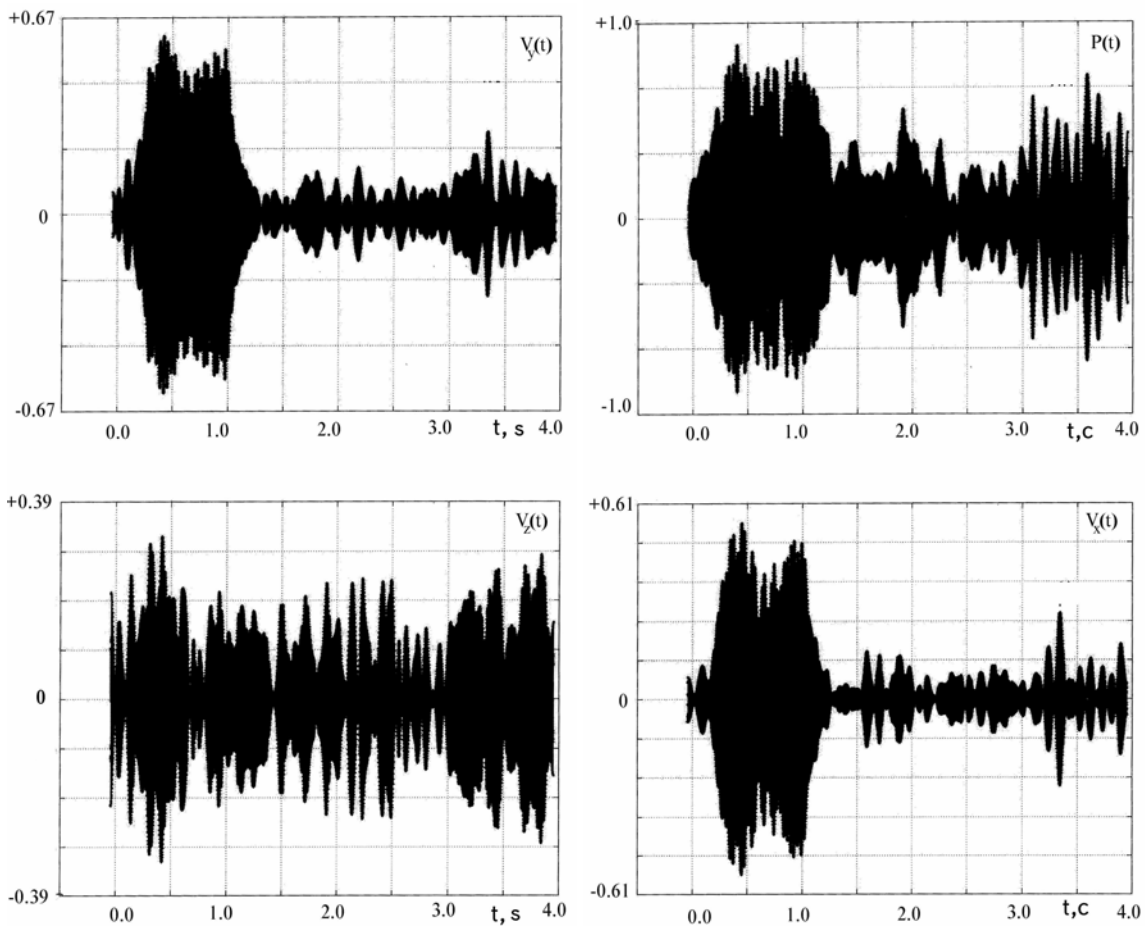


Fig.1 Oscillograms of tone pulse reverberation;  $p(t)$  is the sound pressure,  $V_x(t)$ ,  $V_y(t)$ ,  $V_z(t)$  are orthogonal projections of the particle velocity. Length of the pulse  $\tau=0.9$  s. Inter-pulse separation is 4 s. Depth of the site is 150 m

Consider a case of the surface reverberation. Fig. 3 shows time-dependence of a normalized mean number of arrivals of the surface-scattered pulses over the 0.96-3.41 s time interval at the measurement point, where  $N$  is actual number of arrivals with  $\varphi_0$  and  $t_0$ ; and  $N_0$  is the total number of arrivals over  $2\pi$ , see Fig. 2. Two sectors in the sonogram in Fig. 2,  $\Delta\varphi_1 = 240^\circ-260^\circ$  and  $\Delta\varphi_2 = 260^\circ-280^\circ$ , were chosen as those in which reverberation is originated from the surface scattering.

In Fig. 3A pulses marked with digits arrive precisely from  $250^\circ$  and In Fig. 3B does from  $260^\circ$ , i.e. “sideward” scattering, related to the combined receiver, takes place. The pulses with  $0.1 < n < 0.2$  except pulse 4 in Fig. 3A. Pulses with  $n \approx 0.1$  in the horizontal plane have various bearings within the  $240$ - $280$ -deg sector, the arrivals are irregular in time and the angles of arrival in the vertical plane are in the  $60$ - $80$ -deg sector with respect to horizon. The nature of these irregular pulses can be interpreted the following way. Irregularity thereof with  $n \approx 1$  indicates sound wave backscattering taking place on random irregularities of the surface roughness. Regular signals with  $0.1 < n < 0.2$  are likely to exclusively appear in well-ordered structures. One can suppose, see Refs. 1 and 2 that there exist a certain contribution to the surface roughness that may have properties similar to diffraction lattice. As follows from Fig. 3 and Tab. 2, pulses arrive nearly regularly to the measurement points from  $250^\circ$  and  $260^\circ$ . Absolute error is within  $\pm 0.05$  s.

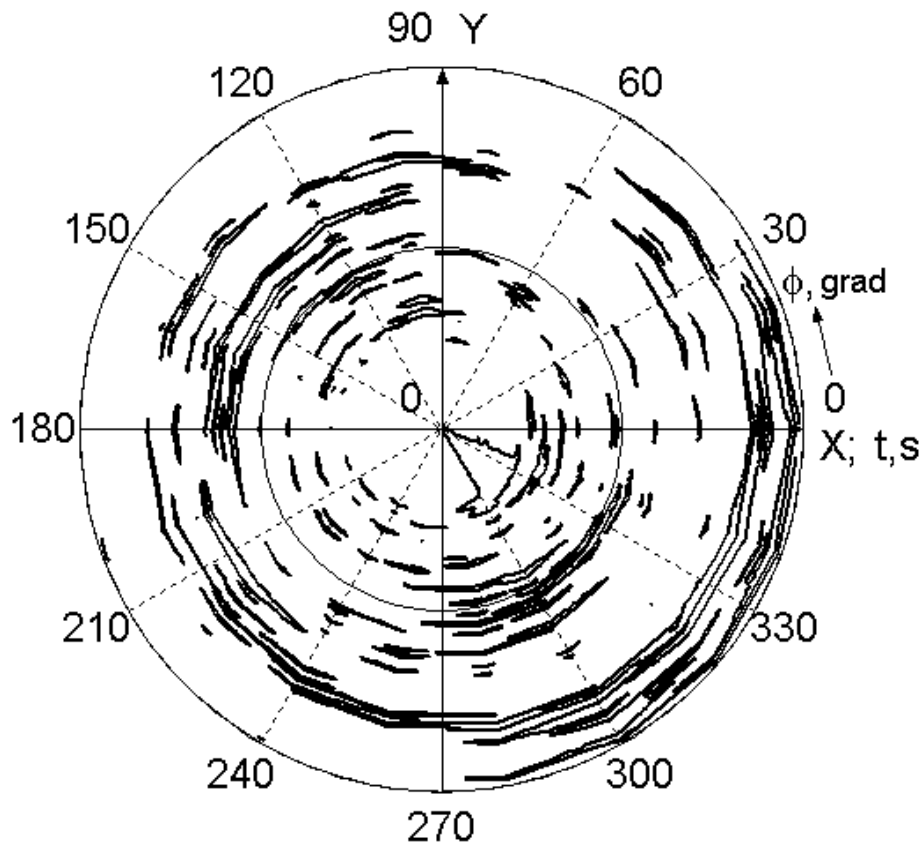


Fig.2 Reverberation polar sonogram in the  $xOy$  plane. The radius is the time from 0 to 4 s. The  $x$  and  $y$  directions are the combined sensor axes. The azimuth  $\phi$  is measured from the  $x$ -direction. The darkness of the sonogram is proportional to the number of pulses with certain  $\phi_0$  and  $t_0$  arrived at the measurement point

Total observation time of 24 measurements is 96 s. Since scattered pulses accumulation during this time gives a stable result, it may be suggested that in each individual event of the surface-roughness-scattering of a pulse, the statistical result of scattering appeared to be independent on a certain time series of the surface waves. The resultant scattering will be dictated by relative arrangement of the transmitter and the sensor, and the direction of surface waves propagation. As seen from the sonogram in Fig. 2, reverberation picture is anisotropic

in the horizontal plane. The steadiest sequence of regular pulses appeared to be found in the 240 to 280-deg sector only.

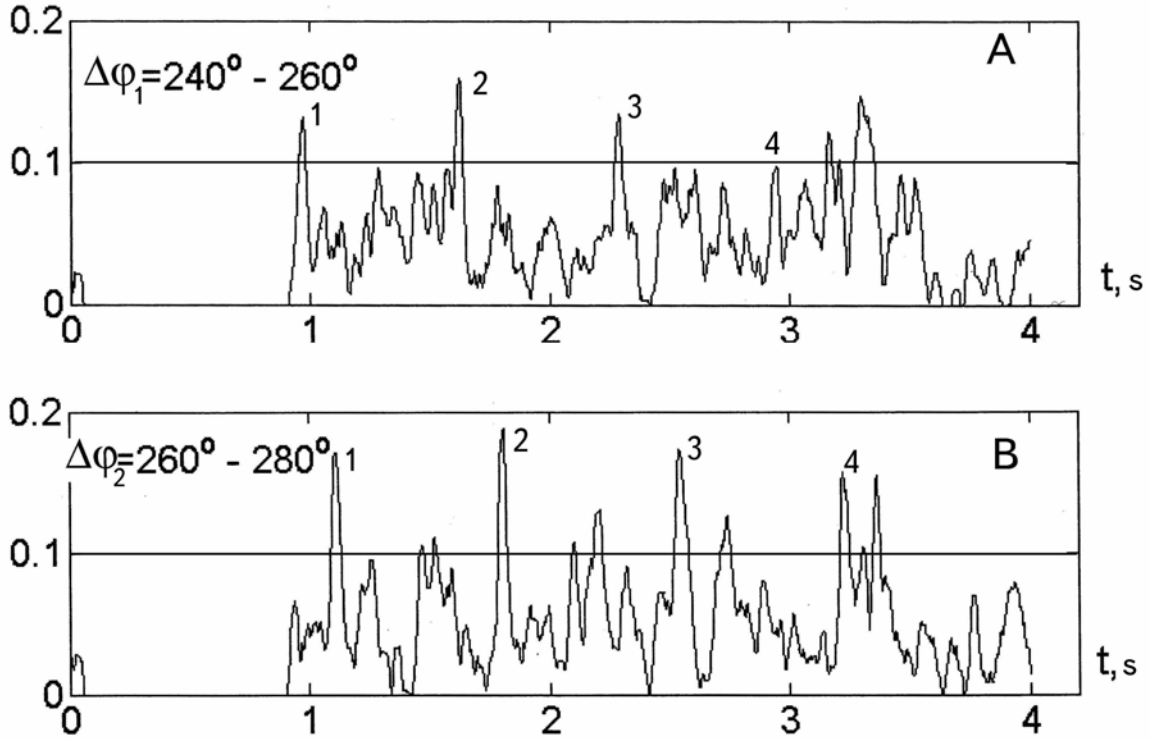


Fig.3 Time-dependence of normalized mean number of scattered pulse arrivals at the measurement point over the 0.96-4.00 s. Plot A for the angular sector  $\Delta\varphi_1 = 240^\circ$ - $260^\circ$ ; plot B for the angular sector  $\Delta\varphi_2 = 260^\circ$ - $280^\circ$ . Data accumulation over 24 sequential time series 4-s long each

Table 3 presents the following characteristics of regular pulses: time separation between pulses with the same number for  $\Delta\varphi_1 = 250^\circ$  and  $\Delta\varphi_2 = 260^\circ$ ; R, the distance from the measurement point to the point of the surface from which scattered pulses come (calculated from  $\Delta t$ );  $\alpha$ , an angle between scattered signal and the horizon in the vertical plane (calculated from R);  $\alpha'$ , angles of scattered signals for 250 or 260-deg directions measured in the experiment.

Making comparison between  $\alpha$  and  $\alpha'$  presented in Tab. 3, one can conclude about qualitative agreement between calculated angle  $\alpha$  and experimentally measured  $\alpha'$ . The grazing angle of the sound wave at the distance of about 3000 m, i.e. rather close to the sensor, can be calculated from  $\sin \chi = \frac{h_0}{R}$ , where  $h_0 = 50$  m is the depth of the transmitter and R is the distance from the transmitter to the scattering point. Ignoring refraction, the grazing angle is about  $1^\circ$ . Under circumstances of the experiment when the grazing angles are small as well as the Rayleigh parameter, the condition for resonant scattering appeared to be met, see Ref. 4,  $\vec{k}_s = \vec{k}_i + \vec{k}_0$ , where  $\vec{k}_s$ ,  $\vec{k}_i$ , and  $\vec{k}_0$  are horizontal projections of the wavenumber vectors related to the scattered, incident and surface roughness wave respectively. Since magnitudes  $k_s = k_i = 2\pi/\lambda$  and the directions of  $\vec{k}_s$  and  $\vec{k}_i$  are known from the experiment, we are able to get  $\vec{k}_0$ . Vector  $\vec{k}_s$  makes an angle  $\gamma_s = 80^\circ$  to the x-axis. Vector  $\vec{k}_i$  in the

scattering point 676 m apart from the sensor makes an angle  $\gamma_s = -54^\circ$  to the x-axis. In doing so, we can calculate the angle between vector  $\vec{k}_0$  and the x-axis to be  $\gamma_0 = -76^\circ$ . Hence,

Tab.2

250°	$\Delta t_{21}=0.65$ s	$\Delta t_{32}=0.65$ s	$\Delta t_{43}=0.66$ s
260°	$\Delta t_{21}=0.70$ s	$\Delta t_{32}=0.75$ s	$\Delta t_{43}=0.66$ s

vector  $\vec{k}_0 = \vec{k}_i - \vec{k}_s$  bisects the angle made by  $\vec{k}_i$  and  $\vec{k}_s$ . Since vector  $\vec{k}_0$  is orthogonal to the surface wave front in the given case, the scattered waves propagation in 250 and 260-deg directions differs not much from possible propagation of rays geometrically reflected from the surface roughness. In that case, as follows from Refs. 1 and 2, scattered sound field is equal to diffraction spectrum. The vector  $\vec{k}_0$  of the surface waves (on which scattering takes place) is rather close to the swell propagation direction. As seen from the Tab. 3, a sequence of regular signals with related times of arrival and angles of scattering comes from the surface points separated by 765 m during 2.11 s. In that case sound wave reflected from the horizontal plane eludes being detected by the sensor.

Tab.3

$\Delta t, s$	R, m	$\alpha$ , deg	$\alpha'$ , deg
0.15	676	13	15±5
0.20	900	10	15±5
0.30	1350	7	10±5
0.32	1441	6	5±5

The diffraction spectrum shape in Fig. 9 in Ref. 2 estimated under conditions close to those in the present experiment are in qualitative agreement with the results presented here. Hence, one can interpret four regular pulses shown in Fig. 3 as lines in the diffraction spectrum when observing low-frequency sound diffraction on the deep ocean surface roughness.

#### 4. CONCLUSIONS

The principle results of the work presented are as follows,

(1) Tone pulse scattering on the surface roughness results in outward-radiating wave with directivity pattern composed of separated energy flux density vector maximums with different grazing angles. The ensemble of these maximums can be interpreted as a diffraction spectrum, i.e. at a certain mutual arrangement of  $\vec{k}_0$  and  $\vec{k}_i$  the surface roughness will possess the properties of a diffraction lattice.

(2) As follows from the experiment done, the surface roughness has spatial and temporal coherence. When the scattering took place over a piece of the sector with sides of 765 and 490 m, regular pulses in the scattered field were observed during 96 s.

(3) Combines receivers application appears to have considerable promise for studying properties of the sound reverberation.

## REFERENCES

- [1] L. Brekhovskikh, Wave diffraction on the rough surface 1, Experimental and Theoretical Physics Journal, Vol. 23, no.3(9), 275-288, 1952 (in Russian)
- [2] L. Brekhovskikh, Wave diffraction on the rough surface 2, Experimental and Theoretical Physics Journal, Vol. 23, no.3(9), 290-304, 1952 (in Russian)
- [3] V. Shchurov, Vector acoustics of the ocean, Dalnauka, 307, Vladivostok, 2003 (in Russian)
- [4] L. Brekhovskikh and Yu. Lysanov, Fundamentals of ocean acoustics, Springer-Verlag-Heidelberg, 250, Berlin-New York